Journal of Solid State Chemistry **153,** 26–29 (2000)
doi:10.1006/jssc.2000.8725, available online at http://www.idealibrary.com on IDEAL®

Synthesis and Structure of Layered Manganese Oxychalcogenides: Sr_2CuMnO_3S and $Sr_4Cu_2Mn_3O_{7.5}Q_2$ (Q = S, Se)

W. J. Zhu and P. H. Hor

Department of Physics and Texas Center for Superconductivity, University of Houston, Houston, Texas 77204-5932

Received October 12, 1999; in revised form March 15, 2000; accepted March 27, 2000; published online June 26, 2000

New layered manganese oxychalcogenides with alternating Cu_2Q_2 and perovskite oxide layers have been synthesized, where the perovskite oxide layers are $(MnO_2)(SrO)(SrO)(MnO_2)$ and $(MnO_2)(SrO)(MnO_{1.5})(SrO)(MnO_2)$ for Sr_2CuMnO_3S and $Sr_4Cu_2Mn_3O_{7.5}Q_2$ (Q = S, Se), respectively. Jahn–Teller distorsion due to Mn^{3+} is evident in both compounds. © 2000 Academic Press

INTRODUCTION

Transition-metal oxides exhibit unusual physical properties such as high-T_c superconductivity and metal–insulator transition. Layered perovskite oxides provide very rich structure varieties for band structure, cation/anion valence, and carrier density modification. The success of this approach has been well demonstrated in the field of high-T_c cuprates (1). Recently we have investigated the transition-metal oxychalcogenide system and identified a family of layered phases with Cu_2Q_2 (Q = S, Se) and perovskite oxide sheets of Cr, Mn, Fe, Co, and Zn (2–4). Those cations assume a square-planar or square-pyramidal oxygen coordination geometry. As part of a continuing investigation of this class of materials, we report here synthesis and structure of new manganese members: Sr_2CuMnO_3S and $Sr_4Cu_2Mn_3O_{7.5}Q_2$ (Q = S, Se).

EXPERIMENTAL PROCEDURES

Sample Sr_2CuMnO_3S was synthesized from SrS, $SrCuO_2$, MnO_2, and Mn in the ratio 1 : 1 : 0.5 : 0.5, while $Sr_4Cu_2Mn_3O_{7.5}Q_2$ (Q = S, Se) were prepared from SrS, $SrCuO_2$, MnO_2, and Mn by 1 : 1 : 0.88 : 0.63 for Q = S and SrO, $SrCuO_2$, Se, MnO_2, and Mn by 1 : 1 : 1 : 0.37 : 1.13 for Q = Se. Materials mixing and grinding were carried out in an argon-filled glovebag. SrO was heated under vacuum before use. Precursor SrS was prepared by hydrogen reduction of $SrSO_4$ at 900°C for 24 h, while $SrCuO_2$ was obtained by reacting $SrCO_3$ with CuO at 920°C. Samples sealed in quartz capsules under vacuum were heated slowly to 800–850°C and held for 12 h. The resulting pellets were reground and retreated one more time. The resulting pellets were dark gray. X-ray diffraction characterization was on a Rigaku-Dmax diffractometer. Intensity data were collected using Cu$K\alpha$ radiation between $2\theta = 15$–$105°$ at steps of 0.02° and counting time of 10 s. The structure model is built on the concept of layer stacking of anti-PbO type Cu_2S_2 and perovskite oxide layers separated by Sr. Initial structure parameters were estimated by the bond valence rule (5). Structure refinement was performed using the DBW-9411 Rietveld program (6) with a pseudo-Voigt peak shape function. Preferred orientation along [001] was corrected using a March–Dollase function. Variables include global and structure parameters, i.e., scale factor, overall thermal parameter, instrument zero point, background function, peak width function, lattice parameters, atomic positions, occupancy, isotropic thermal factors, and preferred function. Temperature dependence of resistivity was measured from 300 to 4.2 K on the polycrystalline samples by the standard four-lead method.

RESULTS AND DISCUSSION

1. Sr_2CuMnO_3S

Single phase was obtained for Sr_2CuMnO_3S. This phase cannot be obtained with Se substitution for S. It is isostructural to Sr_2CuGaO_3S with two square-pyramidal oxide layers alternating with Cu_2S_2 (Fig. 1). Lattice parameters for the tetragonal unit cell was determined to be $a = 3.831(1)$ Å, $c = 15.951(5)$ Å. Rietveld refinement gives good agreement between observed and calculated profiles (Fig. 2) with agreement factors: $R_p = 5.87\%$, $R_{wp} = 8.13\%$, $S = 1.66$, $R_B = 7.69\%$, $R_F = 6.46\%$. Table 1 lists the structure parameters and derived atomic distances. The Mn cation has square pyramidal oxygen coordination geometry with the atomic valence calculated to be 3.00. Its long distance (3.374 Å) from S indicates no significant bonding between them. Due to the Jahn–Teller effect of Mn^{3+}, Mn–O(2) (1.981 Å) is longer than Mn–O(1) (1.938 Å). The substitution of Cu on the Mn site was considered impossible, because the

0022-4596/00 $35.00

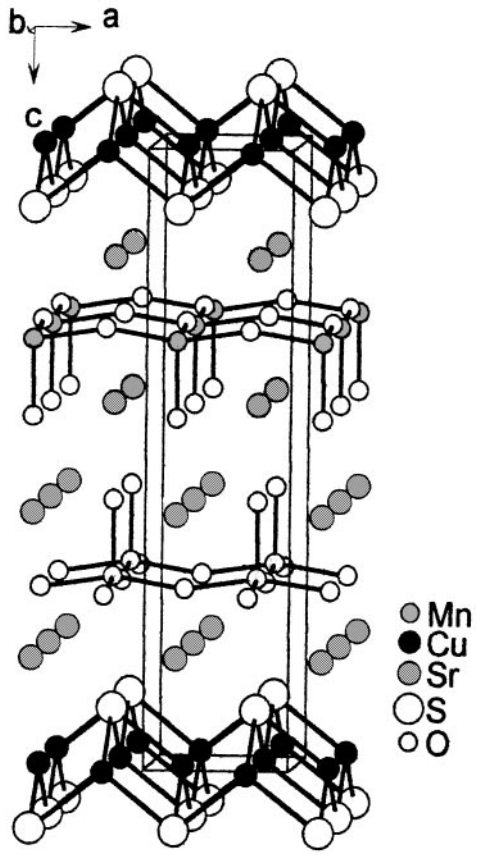

FIG. 1. Structure of Sr_2CuMnO_3S, showing alternately stacking Cu_2S_2 and square-pyramidal MnO_3 layers.

estimated valence is about 2.0 and this species (Cu^{2+}) cannot coexist with the S anion. Similar to other members in this class of materials, the large thermal parameter of Cu was attributed to the slight vacancy at the Cu site. The structure refinement did improve from $R_{wp} = 8.13\%$ to 7.75% and the Cu occupancy reduces to 0.92 when its

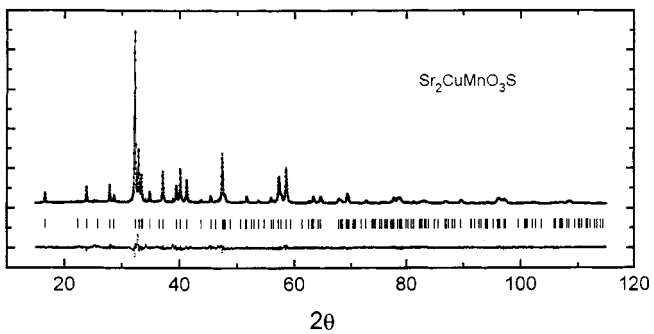

FIG. 2. Observed and calculated X-ray diffraction patterns for Sr_2CuMnO_3S with their difference and Bragg reflection positions shown at the bottom.

TABLE 1
Atomic Coordinates, Thermal Parameters (Å^2), and Selected Atomic Distances for Sr_2CuMnO_3S (Space Group *P4/nmm*)

	x	*y*	*z*	*B*
Mn	$\frac{1}{4}$	$\frac{1}{4}$	0.3038(4)	0.3(1)
Cu	$\frac{1}{4}$	$-\frac{1}{4}$	0	2.4(1)
Sr(1)	$-\frac{1}{4}$	$-\frac{1}{4}$	0.1831(2)	0.5(1)
Sr(2)	$-\frac{1}{4}$	$-\frac{1}{4}$	0.4163(2)	1.0(1)
S	$\frac{1}{4}$	$\frac{1}{4}$	0.0920(5)	2.5(1)
O(1)	$\frac{1}{4}$	$-\frac{1}{4}$	0.2852(7)	1.6(4)
O(2)	$\frac{1}{4}$	$\frac{1}{4}$	0.4279(9)	0.2(3)
Mn–O(1)	1.938(1)		Mn–S	3.378(6)
Mn–O(2)	1.981(9)		Cu–S	2.413(3)

thermal factor was fixed at 0.5 Å^2. This compound exhibits a very high resistivity (over 1 MΩ). Probably due to the short lattice (3.83 Å) along the *a* and *b* axes of the MnO_3 layer as in Sr_2CuMnO_3S, we are unable to synthesize the Se-analogue of this phase.

2. *$Sr_4Cu_2Mn_3O_{7.5}Q_2$ (Q = S, Se)*

A pure phase was obtained for both compounds. All X-ray diffraction peaks were completely indexed on a body-centered tetragonal unit cell. Their lattice parameters were refined to be $a = 3.890(1)$ Å, $c = 34.341(9)$ Å, and $a = 3.888(2)$ Å, $c = 35.29(2)$ Å for Q = S and Se, respectively. Figure 3 shows the structure model where the Cu_2Q_2 layer stacks alternately with the Mn perovskite oxide layer $(MnO_2)(SrO)(MnO_{1.5})(SrO)(MnO_2)$ separated by Sr. Rietveld refinement was performed on structure and global parameters. Oxygen thermal parameters were fixed at 0.8 Å^2, and occupancy of O(3) was refined to a value between 0.71 and 0.74, close to the value 3/4. Good agreement was achieved between the observed and calculated diffraction profiles (Fig. 4). Table 2 gives atomic positional and thermal parameters with the selected atomic distances listed in Table 3. Again the Cu atom shows the relatively large thermal parameter that is a common feature for this class of materials. The Mn perovskite block $(MnO_2)(SrO)(MnO_{1.5})(SrO)(MnO_2)$ is very similar to $(CuO_2)(BaO)(CuO_\delta)(BaO)(CuO_2)$ in $YBa_2Cu_3O_{7-\delta}$. Mn(2)–O(2) is longer than Mn(1)–O(2). Similar to the case of Cu^{2+} in $YBa_2Cu_3O_{7-\delta}$, this structure feature results from the Mn^{3+} Jahn–Teller effect. $Mn^{3+}(2)$ $3d_{Z^2}$ aligns along the *c* axis, while $Mn^{3+}(1)$ $3d_{Z^2}$ orients along the *a* or *b* axis where about one-quarter O(3) site is vacant. Although structure refinement based on X-ray diffraction data cannot determine O(3) vacancy ordering, we can expect that $Mn^{3+}(1)$ also assumes a square-pyramidal oxygen configuration. The apical oxygen and vacancy are located along the *c* axis for Mn(2), while they

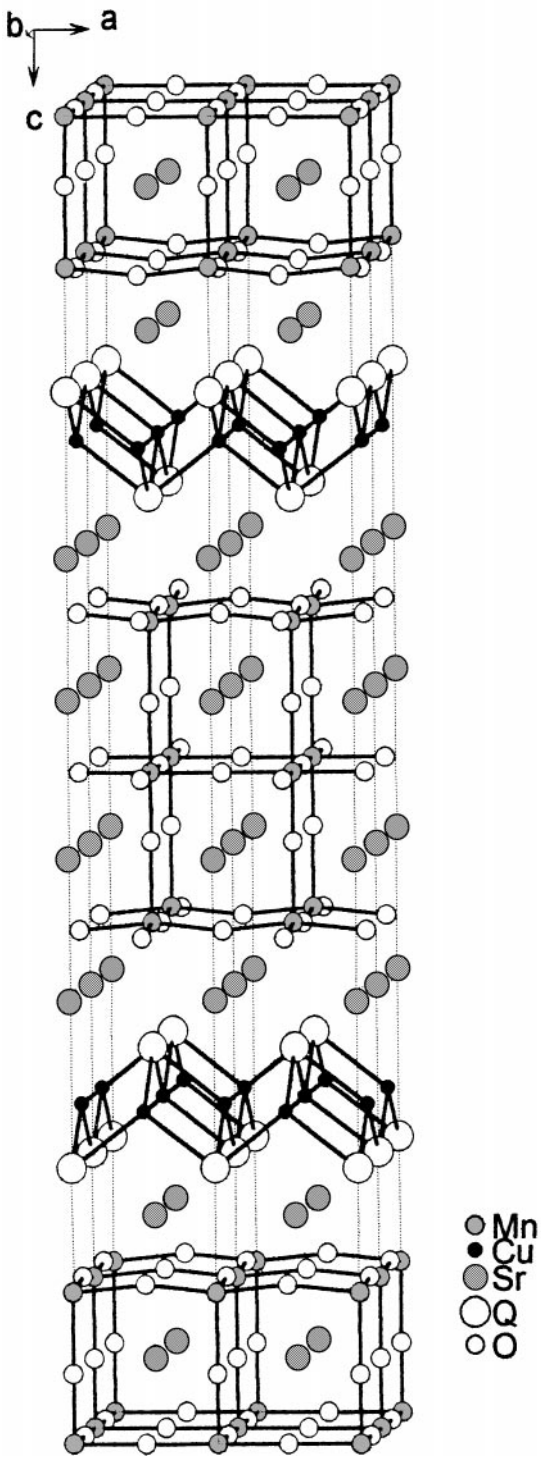

FIG. 3. Structure of $Sr_4Cu_2Mn_3O_{7.5}Q_2$ (Q = S, Se) with the Cu_2Q_2 layer alternating with a triple Mn perovskite oxide layer.

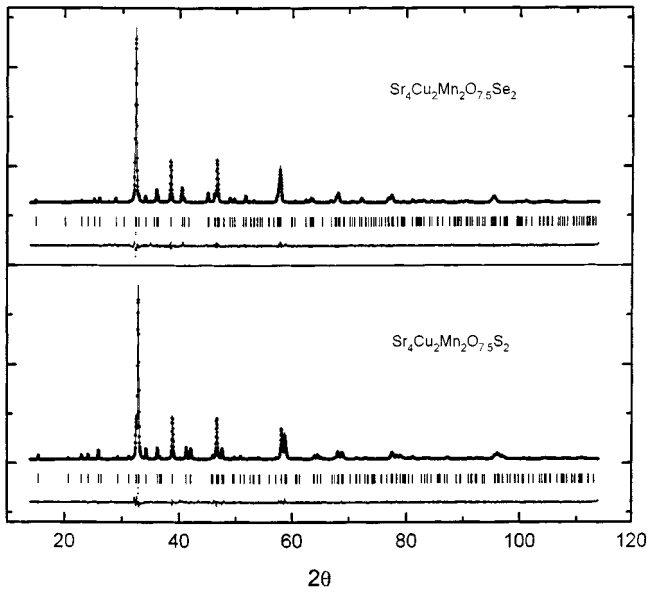

FIG. 4. Observed and calculated X-ray diffraction patterns for $Sr_4Cu_2Mn_3O_{7.5}Q_2$ (Q = S, Se) difference and Bragg reflection positions shown at the bottom.

are within the *ab* plane for Mn(1). By analogy with Cu(1) of the Cu–O chain in $YBa_2Cu_3O_{7-\delta}$, Mn(1) probably can be substituted by various kinds of elements. The partial substitution of Mn^{3+} for Cu^{+} at the Cu^{+} site and Cu^{+} for Mn^{3+} at the Mn(1) site cannot be excluded. Compared with the S-containing compound, the Se-containing phase has a longer *c* axis but with nearly the same *a* and *b* axes. Structure is more rigid in the *ab* plane than along the *c* axis. The Sr(2) plane is pushed farther away from the chalcogen plane along the *c* axis for Q = Se.

Since many manganese perovskite oxides have been known to show metal–insulator transition either by p-type or n-type doping, e.g., $(La,Ca)MnO_3$, $(Ca,Th)MnO_3$, and

TABLE 2
Atomic Coordinates and Thermal Parameters (Å²) for $Sr_4Cu_2Mn_3O_{7.5}Q_2$ (Q = S, Se) (Space Group *I4/mmm*)

			(Q = S)[a]		(Q = Se)[b]	
	x	y	z	B	z	B
Mn(1)	0	0	0	0.4(2)	0	0.5(4)
Mn(2)	0	0	0.1136(2)	0.3(1)	0.1099(1)	0.4(3)
Cu	$\frac{1}{2}$	0	$\frac{1}{4}$	1.6(1)	$\frac{1}{4}$	1.5(3)
Sr(1)	$\frac{1}{2}$	$\frac{1}{2}$	0.0595(1)	0.9(2)	0.0561(3)	0.8(5)
Sr(2)	$\frac{1}{2}$	$\frac{1}{2}$	0.1668(1)	0.3(3)	0.1622(1)	0.5(3)
Q	0	0	0.2076(2)	0.4(1)	0.2052(1)	0.6(3)
O(1)	$\frac{1}{2}$	0	0.1197(3)	0.8	0.1162(3)	0.8
O(2)	0	0	0.0523(4)	0.8	0.0519(5)	0.8
O(3)	$\frac{1}{2}$	0	0	0.8	0	0.8

[a] R_{wp} = 6.97%, R_p = 5.07%, R_E = 5.60%, S = 1.24, R_B = 5.10%, R_F = 4.81% for Q = S.
[b] R_{wp} = 7.63%, R_p = 5.66%, R_E = 5.95%, S = 1.28, R_B = 5.94%, R_F = 5.47% for Q = Se.

TABLE 3
Atomic Distances (Å) for $Sr_4Cu_2Mn_3O_{7.5}Q_2$ (Q = S, Se)

	Q = S	Q = Se
Mn(1)–O(2)	1.796(4)	1.832(5)
Mn(1)–O(3)	1.945(1)	1.944(1)
Mn(2)–O(1)	1.956(2)	1.956(3)
Mn(2)–O(2)	2.105(4)	2.047(5)
Mn(2)–Q	3.228(5)	3.363(6)
Cu–Q	2.430(3)	2.506(4)

$(La,Sr)_{n+1}Mn_nO_{3n+1}$ ($n = 2, 3$), we have attempted La doping for Sr and reducing the oxygen nonstoichiometry. $(La,Sr)MnO_{3-x}$ impurity appears even with slight La substitution. Increasing oxygen content reduces the sample resistivity. The sulfur-containing sample shows higher resistivity than that of the selenium-containing compound. For the Se-containing phase, it is about $10\ \Omega \cdot$cm. Cu deficiency possibly is the source of hole carrier. It is not possible to dope holes on the Mn $3d$ band that lies lower than the S $3p$ and Se $4p$ bands.

In summary, new layered manganese oxychalcogenides Sr_2CuMnO_3S and $Sr_4Cu_2Mn_3O_{7.5}Q_2$ (Q = S, Se) have been synthesized and their structures were determined. The Mn^{3+} cation assumes square-pyramidal oxygen coordination geometry. On the basis of the Mn–O bond lengths determined, it is apparent that Jahn–Teller distortion due to Mn^{3+} exists in both compounds. We are unable to dope the system into the metal–insulator boundary either by introducing more Cu deficiency or by increasing oxygen content.

ACKNOWLEDGMENTS

This work was supported by the Texas Center for Superconductivity at the University of Houston.

REFERENCES

1. B. Raveau *et al.*, "Crystal Chemistry of High-T_c Superconducting Copper Oxides." Springer-Verlag, Berlin, 1991.
2. W. J. Zhu, P. H. Hor, A. J. Jacobson, G. Crisci, T. A. Albright, S. H. Wang, and T. Vogt, *J. Am. Chem. Soc.* **119,** 12388 (1997).
3. W. J. Zhu and P. H. Hor, *Inorg. Chem.* **36,** 3576 (1997).
4. W. J. Zhu and P. H. Hor, *J. Solid State Chem.* **134,** 128 (1997).
5. N. E. Brese and M. O'Keeffe, *Acta Crystallogr. B* **47,** 192 (1991).
6. R. A. Young, A. Sakthivel, T. S. Moss, and C. O. Paiva-Santos, *J. Appl. Crystallogr.* **28,** 366 (1995).